

Original Research



LncRNA uc003pxg.1 Interacts With miR-339-5p Promote Vascular Endothelial Cell Proliferation, Migration and Angiogenesis

Ping Li , MD^{1,2,*}, Feng Wang, MD, PhD^{1,3,*}, Anna Yue, MD^{1,*}, Yanling Xuan, MD⁴, Ying Huang, MD^{1,2}, Jingyi Xu, MD^{1,2}, Jiayi Weng, MD, PhD¹, Yuan Li, MD¹, and Kangyun Sun, MD¹

¹Department of Cardiology, The Affiliated Suzhou Hospital of Nanjing Medical University, Suzhou Municipal Hospital, Gusu School, Nanjing Medical University, Suzhou, P. R. China

²Department of Central Laboratory, The Affiliated Suzhou Hospital of Nanjing Medical University, Suzhou Municipal Hospital, Gusu School, Nanjing Medical University, Suzhou, P. R. China

³Department of Pharmacy, The Affiliated Suzhou Hospital of Nanjing Medical University, Suzhou Municipal Hospital, Gusu School, Nanjing Medical University, Suzhou, P. R. China

⁴The First School of Clinical Medicine, Nanjing University of Chinese Medicine, Nanjing, P. R. China

OPEN ACCESS

Received: May 6, 2024

Revised: Aug 29, 2024

Accepted: Oct 9, 2024

Published online: Nov 18, 2024

Correspondence to

Kangyun Sun, MD

Department of Cardiology, The Affiliated Suzhou Hospital of Nanjing Medical University, 242 Guangji Road, Suzhou 215008, P. R. China.
Email: skywj66@163.com

Yuan Li, MD

Department of Cardiology, The Affiliated Suzhou Hospital of Nanjing Medical University, 242 Guangji Road, Suzhou 215008, P. R. China.
Email: liyuan1596215@163.com

*Ping Li, Feng Wang, and Anna Yue contributed equally to this work.

Copyright © 2025. The Korean Society of Cardiology

This is an Open Access article distributed under the terms of the Creative Commons Attribution Non-Commercial License (<https://creativecommons.org/licenses/by-nc/4.0>) which permits unrestricted noncommercial use, distribution, and reproduction in any medium, provided the original work is properly cited.

ORCID iDs

Ping Li

<https://orcid.org/0000-0003-2692-786X>

AUTHOR'S SUMMARY

Based on the overall experimental data, we speculate that when vascular endothelial cells suffer from harmful stimulation, uc003pxg.1 is upregulated and miR-339-5p is downregulated, leading to upregulated expression of transforming growth factor- β 1, α -smooth muscle actin, CD31, collagen I, collagen III, and endoglin. In turn, the proliferation and migration ability of cells are enhanced, cell mesenchymal transition is enhanced, and collagen deposition and angiogenesis lead to the formation and development of vascular plaques and promote the development of coronary atherosclerosis.

ABSTRACT

Background and Objectives: This study aimed to investigate the roles of lncRNA uc003pxg.1 and miR-339-5p in regulating the occurrence and development of coronary heart disease.

Methods: First, the expression levels of uc003pxg.1 and miR-339-5p were verified in peripheral blood mononuclear cells of clinical samples. Then, the target gene was identified using high-throughput sequencing combined with bioinformatics. Human umbilical vein endothelial cells (HUVECs) were transfected with si-uc003pxg.1, miR-339-5p mimic and miR-339-5p inhibitor, and the expression of related genes was detected by reverse transcription-quantitative polymerase chain reaction and western blotting. EdU, CCK-8, Cell scratch and Transwell assays were used to analyze the effects of uc003pxg.1 and miR-339-5p on cell proliferation and migration.

Results: The expression of uc003pxg.1 and miR-339-5p was negatively correlated in clinical samples and HUVECs. The si-uc003pxg.1 and miR-339-5p mimic decreased the proliferation and migration of HUVECs and decreased the expression of transforming growth factor (TGF)- β 1 and α -smooth muscle actin (SMA). The protein expression levels of TGF- β 1, α -SMA, CD31, collagen I, collagen III and endoglin were decreased, and angiogenesis was weakened. The miR-339-5p inhibitor had the opposite effect.

Funding

This work was supported by the Science and Technology Project of Ke Jiao Xing Wei (KJXW2021039). Specific Disease Cohort Item (GSKY20220406). The Key Discipline of Cardiovascular Disease in Suzhou (SZXK202110). Research on Application of Medical Innovation (SKYD2022129, SKYD2022130). Applied Foundational Research of Medical and Health Care of Suzhou City (grant SKJY2021120), Scientific Research Project of Jiangsu Provincial Health Commission (grant M2021099). National Key Research Program (2021YFC2500600, 2500602).

Conflict of Interest

The authors have no financial conflicts of interest.

Data Sharing Statement

The data generated in this study is available from the corresponding authors upon reasonable request.

Author Contributions

Data curation: Wang F, Xuan Y; Investigation: Yue A, Huang Y, Xu J, Li Y; Project administration: Sun K; Resources: Li P, Weng J, Sun K; Supervision: Li Y; Writing - original draft: Li P; Writing - review & editing: Li P.

Conclusions: Our study revealed that upregulation of uc003pxg.1 and downregulation of miR-339-5p in vitro promote cell proliferation, cell migration and angiogenesis and upregulate the expression of TGF- β 1, α -SMA, CD31, collagen I, collagen III and endoglin, which may lead to the development of vascular atherosclerosis.

Keywords: Coronary heart disease; Long noncoding RNA; Cell proliferation; Cell migration; Angiogenesis

INTRODUCTION

Coronary heart disease (CHD), also known as ischemic heart disease (IHD), is a common type of cardiovascular disease.¹⁾ In the past few decades, CHD has been one of the major causes of morbidity and mortality worldwide,²⁾ resulting in approximately 360,000 deaths in the United States and 1.78 million deaths in Europe each year. The traditional risk factors are hypertension, diabetes, hyperlipidemia, age, male sex, smoking, drinking, obesity³⁾⁴⁾ and obstructive sleep apnea.⁵⁾ CHD is mainly caused by abnormal lipid metabolism in the blood deposited on the originally smooth lining of the artery plaque. According to clinical features, CHD can be divided into ‘acute coronary syndrome’ and ‘chronic coronary syndrome’. Narrowing of the artery cavity and insufficient myocardial blood supply lead to IHD, such as angina pectoris and myocardial infarction.⁶⁾⁷⁾ Vascular endothelial dysfunction, inflammation, age and sex, family history, dyslipidemia, hypertension, smoking, obesity, gout, physical inactivity and other factors are risk factors for the development of atherosclerosis.⁸⁾⁹⁾

Long noncoding RNAs (lncRNAs) are defined as RNA transcripts >200 nucleotides that play important roles in diverse biological processes in atherosclerosis. MicroRNAs (miRNAs) regulate posttranscriptional gene expression and are involved in cardiovascular diseases.¹⁰⁾¹¹⁾ MALAT1/miR-15b-5p/MAPK1 mediates endothelial progenitor cell autophagy and influences CHD through the mTOR signaling pathway.¹²⁾ ANRIL can reduce the expression of miR-181b and regulate the function of vascular endothelial cells through the transforming growth factor (TGF)- β R1/Smad signaling pathway.¹³⁾¹⁴⁾ The lncRNA CDKN2B-AS1/miR-126-5p inhibits the proliferation and accelerates the apoptosis of vascular smooth muscle cells (VSMCs) through the upregulation of PTPN7.¹⁵⁾ STAT3 affects the proliferation of human umbilical vein endothelial cells (HUVECs) and the progression of CHD through CX3CL1/miR-15a-5p.¹⁶⁾ The deposition of lipids, macrophages and collagen and cell proliferation and migration are the main processes of plaque formation.¹⁷⁾ Plaque bleeding can be caused by plaque rupture or angiogenesis bleeding, which can rapidly lead to the development of unstable angina.¹⁶⁾ Meanwhile, endoglin is also involved in plaque formation in vascular endothelial cells.¹⁸⁾

In our previous study, the previously unreported lncRNA uc003pxg.1 was identified,¹⁹⁾ and uc003pxg.1 targets miR-25-5p to regulate cell proliferation and migration.²⁰⁾ The purpose of this study was to further explore the function of uc003pxg.1. We analyzed the correlation of the expression between uc003pxg.1 and miR-339-5p in clinical CHD patients. We sought to determine the molecular mechanism by which uc003pxg.1 affects the phenotype of HUVECs interacting with miR-339-5p. Their target gene TGF- β 1 was screened to analyze how they affect the development of CHD.

METHODS

Ethical statement

The study was approved by the ethics committee of Nanjing Medical University (KL901117), and written informed consent was obtained from the patients and their families.

Study subjects

Sixty clinical blood samples (from 30 patients with coronary artery disease [CAD] and 30 controls aged 45–80 years) were collected from the Department of Cardiology of The Affiliated Suzhou Hospital of Nanjing Medical University (Suzhou, China). The diagnostic criterion for CAD was significant stenosis ($\geq 50\%$) of at least one segment of the major coronary artery (including the left anterior descending artery, left circumflex artery or right coronary artery). The exclusion criteria were patients with severe primary disease, myocardial infarction, cerebral infarction, acute infection, prior coronary artery bypass, dialysis, cancer, or alcohol or drug abuse. The 30 control cases were selected from routine health examinations. The normal reference intervals of blood tests were as follows: blood pressure, 90–140/60–90 mmHg; blood glucose, 4–6.1 mmol/L; total cholesterol (TC), 2.8–5.7 mmol/L; triglycerides, 0.56–1.7 mmol/L; cholesterol lipids, 2.8–5.17 mmol/L; low-density lipoprotein (LDL), < 3.37 mmol/L; high-density lipoprotein (HDL), 1–2 mmol/L; very LDL, 0.21–0.78 mmol/L; lipoprotein A (LPPA), 0–300 mg/L; cholinesterase, 4.3–10.5 U/L; and total bile acid, 0.1–10 $\mu\text{mol/L}$.

Cell culture and transfection

HUVECs (341788) were purchased from BeNa Culture Collection and cultured in endothelial cell medium (ScienCell, Carlsbad, CA, USA) containing 5% fetal bovine serum, endothelial cell growth additive, streptomycin and penicillin. Cell culture plates were covered with 0.1% gelatin (V900863-100G, Sigma-Aldrich, St. Louis, MO, USA) and incubated for 30 minutes in the incubator, and the supernatant was discarded. Then, the cells were cultured in cell culture plates and placed in a humidified incubator under a 37°C atmosphere with 5% CO₂. Prior to use, the cells were washed with phosphate buffered saline (PBS, HyClone, Cytiva, Marlborough, MA, USA) and digested with a Trypsin-EDTA solution (Millipore Sigma, Burlington, MA, USA). For transfection, HUVECs were seeded at up to 50% confluence in a plate at 24-hour pre-transfection. Subsequently, the cells were transfected with 50 nM small interfering (si)RNA targeting the lncRNA uc003pxg.1 (si-uc003pxg.1), miR-339-5p mimic, miR-339-5p inhibitor and corresponding NC (Guangzhou RiboBio Co., Ltd., Guangzhou, China) using a riboFECT™ CP Transfection kit (Guangzhou RiboBio Co., Ltd.). A total of 2.5 μL siRNA was diluted with 30 μL of 1×riboFECT™ CP Buffer and gently mixed. Subsequently, 3 μL riboFECT™ CP Reagent was added and mixed gently, and the plates were incubated for 15 minutes at room temperature. Then, the transfection complexes were added to the medium. The culture medium was changed at 12 hours, and the cells were incubated for 24–72 hours at 37°C with 5% CO₂. The cells were collected at 24 and 48 hours post-transfection for use in reverse transcription-quantitative reverse transcription-quantitative polymerase chain reaction and western blot analyses, respectively. The oligomer sequences were as follows: si-uc003pxg.1: 5'-GCAATGTAGT CACCAATAA-3'; si-NC: 5'-GGCTCTAGAAAAGCCTATGC-3'; miRNA mimic NC: 5'-UCACAACCUCCUAGAAAGAGUAGA-3'; miRNA inhibitor NC: 5'-UCACA ACCUCCUAGAAAGAGUAGA-3'; miR-339-5p mimic sense: 5'-UC CCUGUCCUCCAGGAGCUCACG-3' and antisense: 5'-CGUGAGCUCCUGGAG GACAGGGA-3'; and miR-339-5p inhibitor: 5'-CGUGAGCUCCUGGAGGACAGG GA-3'.

Peripheral blood mononuclear cell isolation, RNA extraction and reverse transcription-quantitative polymerase chain reaction

Blood samples (4–6 mL) from each participant were collected with EDTA vacuum anticoagulant tubes. The plasma was collected after centrifugation at 1,600× g for 10 minutes to remove the debris. Peripheral blood mononuclear cells (PBMCs) were isolated from blood by gradient centrifugation with Ficoll reagent (GE Healthcare, Chicago, IL, USA).

Total RNA was extracted from PBMCs and cells with TRIzol® Reagent (Ambion, Austin, TX, USA). RNA was reverse transcribed into cDNA with 5× PrimeScript™ RT Master Mix (RR036A, Takara Bio, Inc., Kusatsu, Japan). The reverse transcription reaction conditions were 37°C for 15 minutes, 85°C for 5 seconds, and 4°C for ∞. Fluorescence quantitative real-time polymerase chain reaction (Q-PCR) was performed using SYBR® Premix Ex Taq™ II (RR820A, Takara Bio, Inc.). Q-PCR was performed with a LightCycler® 480 Instrument II Real-Time PCR Detection system (Roche Diagnostics, Rotkreuz, Switzerland). The PCR parameters were 95°C for 30 seconds; 40 cycles of 95°C for 5 seconds and 60°C for 20 seconds; 95°C for 0 seconds, 65°C for 15 seconds and 95°C for 0 seconds. β-Actin served as the internal reference. The primers used in this experiment are shown in Table 1. The primers were synthesized by GENEWIZ Company (Suzhou, China). For miRNA quantification, bulge-loop RT primers and Q-PCR primers specific for miR-339-5p were designed and synthesized by Guangzhou RiboBio Co., Ltd. U6 was used as the internal control. *Ki67* and *Bcl2* were used to detect the expression of genes related to proliferation and apoptosis. All measurements were performed in triplicate. The relative expression data were analyzed with the formula $2^{-\Delta\Delta C_q}$.²¹⁾ Analyses of the different expression levels were performed using GraphPad Prism 7 (GraphPad Software, Inc., San Diego, CA, USA).

Dual-luciferase reporter gene assay

The uc003pxg.1 fragment containing the miR-339-5p binding site was synthesized, cloned and inserted into the target pmirGLO dual-luciferase reporter gene vector; this construct was called pmirGLO-uc003pxg.1-wt. The uc003pxg.1 sequence containing a mutated miR-339-5p binding site was synthesized into the vector, and this construct was called pmirGLO-uc003pxg.1-mut. Gene synthesis and cloning were performed by GENEWIZ Company. HUVECs in 24-well plates were transfected with miR-339-5p mimic or NC mimic and then with pmirGLO-uc003pxg.1-wt or pmirGLO-uc003pxg.1-mut. Lipo3000 (Invitrogen, Thermo Fisher Scientific Inc., Waltham, MA, USA) was used as the transfection reagent. Luciferase activity was measured with a dual-luciferase reporter assay system (E1910) (Promega Co., Ltd., Madison, WI, USA). Fluorescence data were read using a Varioskan LUX (Thermo Scientific, Singapore).

Table 1. Sequences of the primers used in the experiment

Gene	Primer sequence
uc003pxg.1	F: 5'-GTTACCGAAAGCGTTGCCA-3' R: 5'-TATACTCAGTCCAGCAGCCC-3'
TGF-β1	F: 5'-ACCACACCCAGCCCTGTTC-3' R: 5'-CGTCAGCACCAGTAGCCA-3'
α-SMA	F: 5'-GCACGCGACTTCTCAGG-3' R: 5'-TCAGTTTACGATGGCAGCA-3'
Ki67	F: 5'-ACCTGACAGACCTCAAGAGC-3' R: 5'-CTTTGGTGCCTTGGCATGAT-3'
Bcl2	F: 5'-GCCCTGTGGATGACTGAGTA-3' R: 5'-GAAATCAAACAGAGGCCGCA-3'
β-Actin	F: 5'-CACGAACTACCTTCAACTCC-3' R: 5'-CATACTCCTGCTTGCTGATC-3'

F = forward; R = reverse; TGF-β1 = transforming growth factor-β1; α-SMA = α-smooth muscle actin.

Cell proliferation

A CCK-8 kit (Dojindo Laboratories, Kumamoto, Japan) was used to detect cell proliferation. After 12–24 hours of transfection with 50 nm siRNA, 1,000 HUVECs (100 μ L cell suspension) were seeded in each well of a 96-well plate. Ten microliters of CCK-8 solution were added to each well, and the plates were incubated in a 37°C incubator with 5% CO₂ for 2–4 hours. The absorbance at 450 nm was determined by Varioskan LUX (Thermo Scientific).

EdU assay

HUVECs in 24-well plates were covered with round coverslips and grown to an inoculation density of approximately 60% overnight. After transfection with 50 nm NC, si-uc003pxg.1, miR-339-5p mimic and miR-339-5p inhibitor for approximately 48 hours, the cells were washed with PBS, fixed with 4% paraformaldehyde (BL539A, Biosharp, Hefei, China) for 30 minutes, and then treated with 0.5% Triton X-100/PBS solution for 10 minutes to perforate the cell membrane. A Cell-Light EdU Apollo567 in Vitro Flow Cytometry Kit (Guangzhou RiboBio Co., Ltd.) was used for the EdU experiment. 1×Apollo was used to incubate the cells for 30 minutes in the dark, and the cells were then stained with 1×Hoechst for 30 minutes. Images were obtained with the 40× objective lens of a fluorescence confocal microscope (LSM900; Zeiss, Jena, Germany).

Transwell assay

HUVECs were grown to a density of approximately 60% in a 24-well plate overnight and then transfected with 50 nm NC, si-uc003pxg.1, miR-339-5p mimic and miR-339-5p inhibitor for 24 hours. 24-well, 8.0- μ m pore membranes (Corning, Corning, NY, USA) were used in this experiment. A total of 4×10⁴ cells were seeded in the upper chamber in 200 μ L of serum-free medium, 600–800 μ L culture medium containing 10% serum was added to the lower chamber at the same time, and the plates were incubated for 24 hours at 37°C. Then, the cells were fixed with 4% paraformaldehyde for 30 minutes and stained with crystal violet solution for 15 to 30 minutes at room temperature. The cells on the upper membrane surface were gently wiped with cotton swabs. The cells that passed through the membranes were photographed by inverted fluorescence microscopy (OLYMPUS IX73P1F, Olympus, Tokyo, Japan).

Cell scratch assay

Cell migration was studied by scratch assay. Twenty-four hours after transfection of HUVECs in the 6-well plate, the cell aggregation density reached about 90%. A vertical line was quickly and evenly drawn on the dish with a pipette tip of 100 μ L along a ruler. Dead cells were removed by washing with PBS, the initial scratches were photographed using an inverted microscope. The cells continued to be cultured for 24 hours, the dead cells were removed by PBS, and the images were taken again by inverted fluorescence microscopy (OLYMPUS IX73P1F, Olympus). The width of scratch wound was calculated with ImageJ software (National Institutes of Health, Bethesda, MD, USA).

Cell cycle analysis

After the HUVECs were transfected for 48 hours in 6-well plates, the cells were digested with trypsin and washed with PBS. Then, the cells were fixed with 70% cold ethanol for over 24 hours at –20°C. Each sample was stained with the Cell Cycle and Apoptosis Analysis Kit (Beyotime, Shanghai, China) at 37°C for 30 minutes. The cells were washed with cold PBS again, and cell fluorescence data were collected at 488 nm using the PE channel of a flow cytometer (BD FACSCanto II, BD Biosciences, Franklin Lakes, NJ, USA).

Apoptosis assays

The apoptosis rate was detected using an Annexin V-FITC/PI apoptosis kit. Cells were seeded into 6-well plates with a coverage rate of approximately 50–60%. At 24 hours after transfection with 50 nm NC, si-uc003pxg.1, miR-339-5p mimic, and miR-339-5p inhibitor, the culture medium was changed. Cells were collected by trypsin digestion 48 hours after transfection, washed with PBS, and resuspended in 100 μ L of 1 \times binding buffer. Then, 5 μ L of Annexin V-FITC and 5 μ L of PI were added to the resuspended cells, and they were incubated for 15 minutes at room temperature in the dark. Finally, 400 μ L of 1 \times binding buffer was added, and data were collected by flow cytometry (BD FACSCanto II, BD Biosciences) within 1 hour.

High-throughput sequencing and bioinformatics analysis

After transfection mimic NC and miR-339-5p mimic into HUVEC cells for 24 hours, 1 mL Trizol was used to collect cells, and 2 repeats were collected from each group for high-throughput transcriptome sequencing by Ruibo Biotechnology Co., Ltd. (Changzhou, China). The original data obtained by Illumina HiSeq TM 2500. Then calculated the mRNA expression level, analyze mRNA cluster expression. The differentially expressed mRNAs were enriched by Gene Ontology and Kyoto Encyclopedia of Genes and Genomes biological pathways. The target genes of miR-339-5p were predicted by bioinformatics software miRDB, miRWalk, TargetScan and miRTarBase.

Western blotting

After 48 hours of transfection of HUVECs with 50 nm NC, si-uc003pxg.1, miR-339-5p mimic, or miR-339-5p inhibitor in 6-well plates, proteins were extracted using RIPA supplemented with protease inhibitor. Approximately 20–40 μ g of protein was separated using an sodium dodecyl sulfate-polyacrylamide gel (Epizyme Biotech, Shanghai, China) and electrophoresis apparatus (Bio-Rad, Hercules, CA, USA). Then, the protein was transferred to a 0.2 μ m PVDF membrane (Immobilon[®]-PSQ, Sigma-Aldrich, Wicklow, Ireland). The membranes were blocked with 5% skim milk and incubated with rabbit anti-TGF- β 1 (1:1,000, Proteintech, Wuhan, China), anti-CD31 (1:5,000, Proteintech), anti-Endoglin (1:1,000, Proteintech), anti-Collagen I (1:1,000, ABclonal, Wuhan, China), and anti-Collagen III (1:1,000, Immunoway, Suzhou, China) antibodies overnight at 4°C. The secondary antibody was diluted with 5% skim milk and incubated with the membrane for 1 hour at room temperature. After washing the membrane 3 \times 10 minutes with TBST washing buffer, the expression levels of proteins were detected by an automatic chemiluminescence image analyzer (Tanon 5200Multi, Tanon, Shanghai, China) using TanonTM High-sig ECL Western Blotting Substrate (Tanon).

Tube formation assay

HUVECs were cultured in a 24-well plate and treated with 50 nm NC, si-uc003pxg.1, miR-339-5p mimic, and miR-339-5p inhibitor for 24 hours. Matrigel was transferred from a -20°C freezer to a 4°C refrigerator, and the tips were precooled one day in advance. Then, 80 μ L/well Matrigel was added gently along the wall of each well of a 96-well plate, and the plate was incubated at 37°C for 30 minutes. A 1.5 \times 10⁵ cells/mL suspension was prepared, and 1.5 \times 10⁴ cells/well were inoculated into a 96-well plate covered with matrigel. Cell tubule formation occurred after 24 hours, and photos were taken by inverted fluorescence microscopy (OLYMPUS IX73P1F, Olympus).

Cell immunofluorescence assay

The transfected cells were inoculated in 24-well plate with cell crawling tablets (Shanghai, China). After transfection for 24 days, 4% paraformaldehyde (Biosharp) fixed the cells

for 15 minutes. Then the cells were permeated with 0.5% triton 100 for 20 minutes at room temperature, blocked with 5% BSA for 1 hour. Incubated with primary antibody at 4°C overnight. The primary antibody was discarded and soaked with 1×PBST 3 times the second day. The corresponding secondary antibody was added (rabbit, ab150077, Abcam, Cambridge, UK; mouse, ab150116, Abcam) and incubated for 1 hour in dark at room temperature, soaked in 1×PBST for 3 times. Incubated with 1×DAPI for 30 minutes in dark and soaked in 1×PBST for 3 times. Drop 10 µL glycerin in the middle of the slide, carefully remove the 24-well slide with tweezers and needle tips, place the cell surface on the side of the glycerin, sealed the film along the edge with transparent nail polish. Images were obtained with the 20× objective lens of a fluorescence confocal microscope (LSM900, Zeiss) with 488 nm, 594 nm and 405 nm.

Statistical analyses

GraphPad Prism 7 (GraphPad Software, Inc.) was used for data analysis and gene expression correlation. The results are given as the mean ± standard deviation. A 2-tailed Student's t-test was used for normally distributed variables, and one-way analysis of variance followed by multiple comparisons was used when appropriate. The grayscale of western blotting was calculated by ImageJ software (National Institutes of Health). A p value <0.05 was considered statistically significant.

RESULTS

Clinical index information of 60 clinical samples

Detailed data statistics are shown in **Table 2**. The levels of blood pressure, TC, LDL and LPPA in CHD patients were higher than those in the normal group, and the HDL level was lower than that in the normal group. The number of male patients with CHD was 67%, and there were more male patients than female patients.

Table 2. Clinical characteristics of the study subjects

Variable	CON (n=30)	CAD (n=30)	p value
Age (years)	62.8±2.22	63.3±2.38	0.8704
Sex (male)	15 (50.0%)	20 (66.7%)	0.1904
BMI (kg/m ²)	25.85±0.76	25.34±0.51	0.5768
Smoking	8 (26.7%)	14 (46.7%)	0.1080
Drinking	4 (13.3%)	6 (20.0%)	0.4884
Diabetes	6 (20.0%)	11 (36.7%)	0.1520
Hypertension	12 (40.0%)	26 (86.7%)	0.0002 [‡]
TC (mmol/L)	3.29±0.08	4.11±0.19	0.0002 [‡]
TG (mmol/L)	1.72±0.18	1.52±0.12	0.3637
HDL (mmol/L)	1.17±0.06	1.02±0.06	0.0682
LDL (mmol/L)	2.12±0.07	2.45±0.12	0.0231 [*]
VLDL (mmol/L)	0.38±0.04	0.55±0.14	0.2279
LppA (mg/L)	115.7±19.47	287±50.48	0.0025 [†]
ChE (U/L)	7.41±0.29	7.92±0.31	0.2428
TBA (µmol/L)	5.97±1.11	6.97±1.03	0.5128

Values are presented as mean ± standard deviation or numbers of patients (%). The p value was analyzed with Student's t-test.

BMI = body mass index; ChE = cholinesterase; HDL = high-density lipoprotein; LDL = low-density lipoprotein; LppA = lipoprotein A; TBA = total bile acid; TC = total cholesterol; TG = triglyceride; VLDL = very low-density lipoprotein.

^{*}p<0.05, [†]p<0.01, [‡]p<0.001 were regarded as significant.

The expression of the long noncoding RNA uc003pxg.1 was negatively correlated with miR-339-5p

The expression of uc003pxg.1 was significantly upregulated (**Figure 1A**), while miR-339-5p was significantly downregulated (**Figure 1B**) in the PBMCs of 30 CAD patients compared with 30 normal controls, and the expression of uc003pxg.1 was negatively correlated with miR-339-5p (**Figure 1C**). HUVECs were transfected with si-uc003pxg.1, and the uc003pxg.1 was significantly knocked down (**Figure 1D**), the expression of miR-339-5p was significantly upregulated (**Figure 1E**). There was a core region of base complement between uc003pxg.1 and miR-339-5p, and the luciferase activity of the miR-339-5p mimic + uc003pxg.1-wt group was decreased compared with that of the NC group, whereas no significant differences in the luciferase activities were observed between the miR-339-5p mimic and NC samples in the mut group (**Figure 1F**). These results indicated that uc003pxg.1 was negatively correlated with miR-339-5p.

The long noncoding RNA uc003pxg.1 and miR-339-5p affect the proliferation and migration of endothelial cells

After HUVECs were transfected with si-uc003pxg.1 or miR-339-5p mimic, the EdU results showed that the number of HUVECs was decreased. The miR-339-5p inhibitor promoted cell proliferation (**Figure 2A and B**). CCK-8 data also showed that si-uc003pxg.1 and miR-339-5p mimic inhibited the growth of cells, and miR-339-5p inhibitor promoted the growth of cells; these significant differences started at 24 hours (**Figure 2C**). At the same time, si-uc003pxg.1 and miR-339-5p mimic weakened cell migration ability, and miR-339-5p inhibitor enhanced cell migration ability. The effect of miR-339-5p on cell proliferation and migration was more obvious than that of uc003pxg.1 (**Figure 2D-G**).

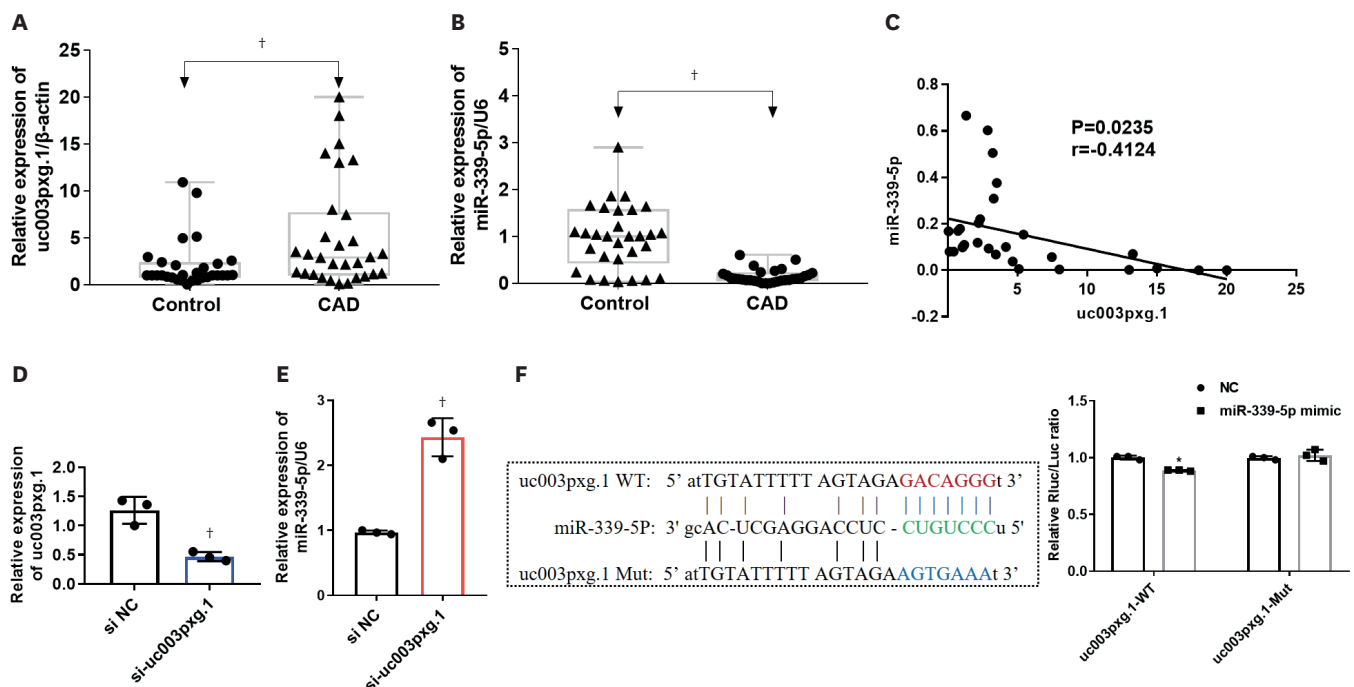


Figure 1. Correlation analysis between uc003pxg.1 and miR-339-5p. (A) Comparison of uc003pxg.1 expression in PBMCs between normal and CAD cases. (B) Comparison of miR-339-5p expression in PBMCs between normal and CAD cases. (C) Correlation analysis of the expression of uc003pxg.1 and miR-339-5p in clinical PBMCs. (D) Expression level of uc003pxg.1 after si-uc003pxg.1 was transfected into HUVECs. (E) Expression level of miR-339-5p after si-uc003pxg.1 was transfected into HUVECs. (F) The interaction between uc003pxg.1 and miR-339-5p was analyzed with a luciferase reporter assay.

CAD = coronary artery disease; HUVEC = human umbilical vein endothelial cell; NC = not control; PBMC = peripheral blood mononuclear cell.

* $p < 0.05$, † $p < 0.01$.

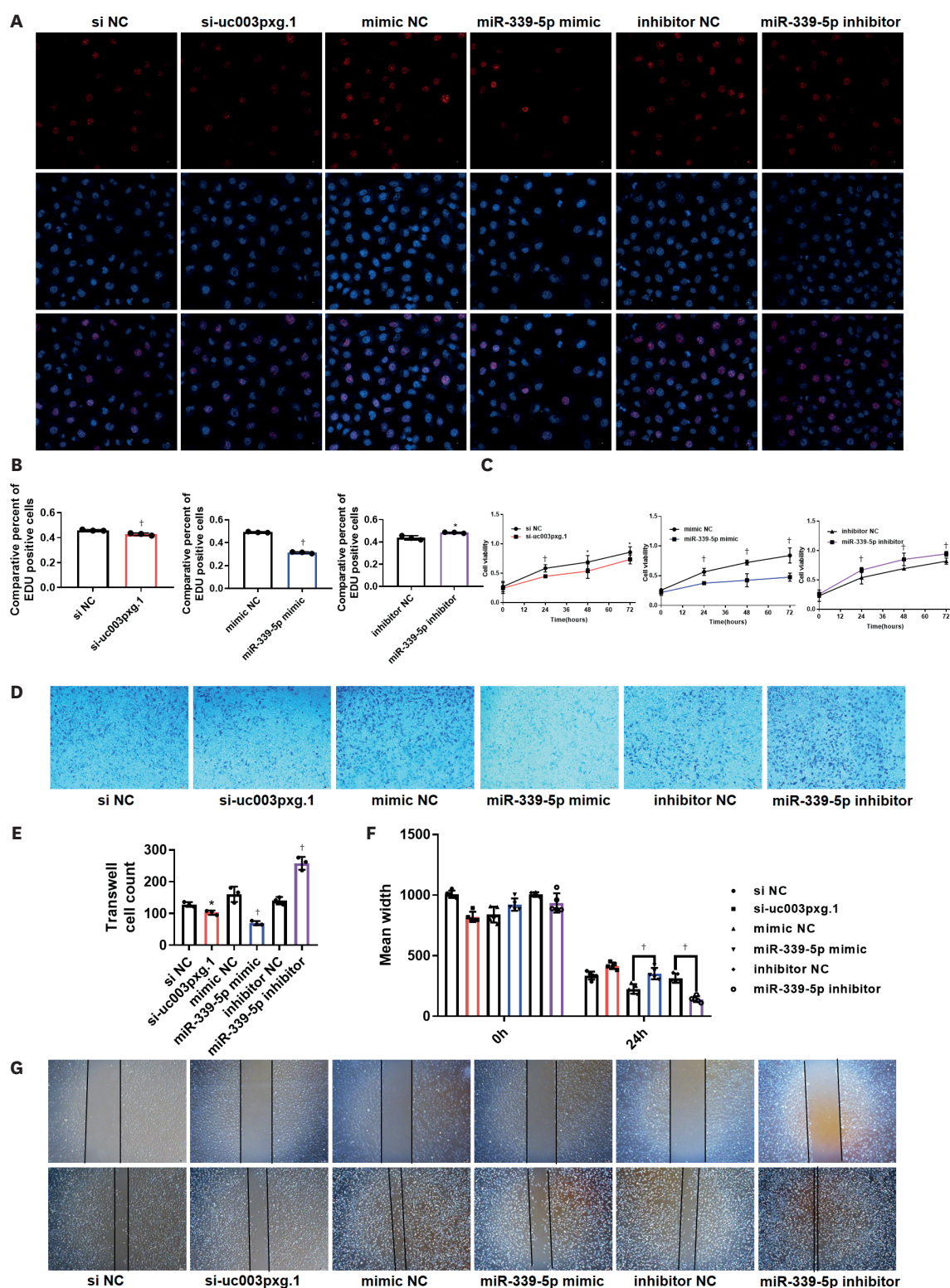


Figure 2. LncRNA uc003pxg.1 and miR-339-5p affected cell proliferation and migration. (A) The effects of si-uc003pxg.1, miR-339-5p mimic, and miR-339-5p inhibitor on the proliferation of HUVECs were analyzed with EdU staining. Red: EDU staining the nuclear of proliferating cells; Blue: Hoechst staining the nuclear of all cells. (B) The rate statistics of EDU positive cells in (A). (C) Cell viability was determined by a cell counting kit-8 assay. (D) The effects of uc003pxg.1, miR-339-5p mimic, and miR-339-5p inhibitor on the migration ability of HUVECs were detected by transwell assay. (E) Transwell data statistics of (D). (F) The width statistics of cell scratch data in (G). (G) The migration ability of HUVECs were detected by cell scratch assay. HUVEC = human umbilical vein endothelial cell; lncRNA = long noncoding RNA; NC = not control. * $p < 0.05$, † $p < 0.01$.

The long noncoding RNA uc003pxg.1 and miR-339-5p affected the cell cycle and apoptosis

After HUVECs were transfected with si-uc003pxg.1 or miR-339-5p mimic, the G2 phase of the cell cycle was significantly decreased compared with the not control (NC) group, and the cells in G2 phase were significantly increased in the miR-339-5p inhibitor group (**Figure 3A and C**). The number of apoptotic cells in the si-uc003pxg.1 and miR-339-5p mimic groups was higher than that in the NC group, while the number of apoptotic cells in the miR-339-5p inhibitor group was lower than that in the NC group (**Figure 3B**). Meanwhile, the related gene *Ki67* and *Bcl2* were down-regulated in the si-uc003pxg.1 and miR-339-5p mimic groups compared with NC groups, and up-regulated in miR-339-5p inhibitor group compared with NC (**Figure 3D**). Moreover, the effect of miR-339-5p on the cell cycle and apoptosis was more significant than that of uc003pxg.1.

Predicted target genes of miR-339-5p by high-throughput sequencing

After HUVECs were transfected with mimic NC and miR-339-5p mimic for approximately 24 hours, the cells were collected with TRIzol, RNA was extracted for high-throughput sequencing at Guangzhou RiboBio Co., Ltd., and the sequencing results were analyzed. Cluster analysis showed that the miR-339-5p mimic group had significant gene expression differences compared with the NC mimic group, and there are obvious distinctions among 2 groups (**Figure 4A**). The volcano map also showed that the miR-339-5p mimic group had 3,168 upregulated mRNAs and 2,055 downregulated mRNAs compared with the NC mimic group (**Figure 4B**). Genes of the TGF- β 1 pathway were among the downregulated genes identified by sequencing (**Figure 4C-E**). The target genes of miR-339-5p were predicted with the bioinformatics software programs miRDB, miRWalk, TargetScan, and miRTarBase, and miR-339-5p exhibited targeted binding with TGF- β 1 (**Figure 4F**).

The long noncoding RNA uc003pxg.1 and miR-339-5p affect the expression of mesenchymal transition-related genes in endothelial cells

The expression of miR-339-5p was inhibited by approximately 50% by the miR-339-5p inhibitor, and the enhanced expression of the mimic was high-efficiency (**Figure 5A**). After transfection for approximately 24 hours, the expression levels of α -smooth muscle actin (SMA) and TGF- β 1 were downregulated in the si-uc003pxg.1 and miR-339-5p mimic groups compared with the NC group and were upregulated in the miR-339-5p inhibitor group compared with the NC group (**Figure 5B**). The luciferase activity of the miR-339-5p mimic + TGF- β 1-wt group was decreased compared with that of the NC group, whereas there were no significant differences between the miR-339-5p mimic+ TGF- β 1-mut and NC groups (**Figure 5C**). This finding indicates that there is an interaction between TGF- β 1 and miR-339-5p. Meanwhile, the western blotting results also showed that CD31, collagen III, collagen I, endoglin, and TGF- β 1 were downregulated in the si-uc003pxg.1 and miR-339-5p mimic groups compared with the NC group. However, they were upregulated in the miR-339-5p inhibitor group compared with the NC group (**Figure 5D and E**). The results of cell immunofluorescence experiments also showed that si-uc003pxg.1 and miR-339-5p mimic inhibited the expression of α -SMA and CD31, whereas miR-339-5p inhibitor promoted their expression (**Supplementary Figure 1**).

The long noncoding RNA uc003pxg.1 and miR-339-5p participate in the development of coronary heart disease by affecting angiogenesis

After HUVECs were transfected with si-uc003pxg.1 or miR-339-5p mimic, the vascular tubular formation ability was significantly weakened compared with that of the NC group.

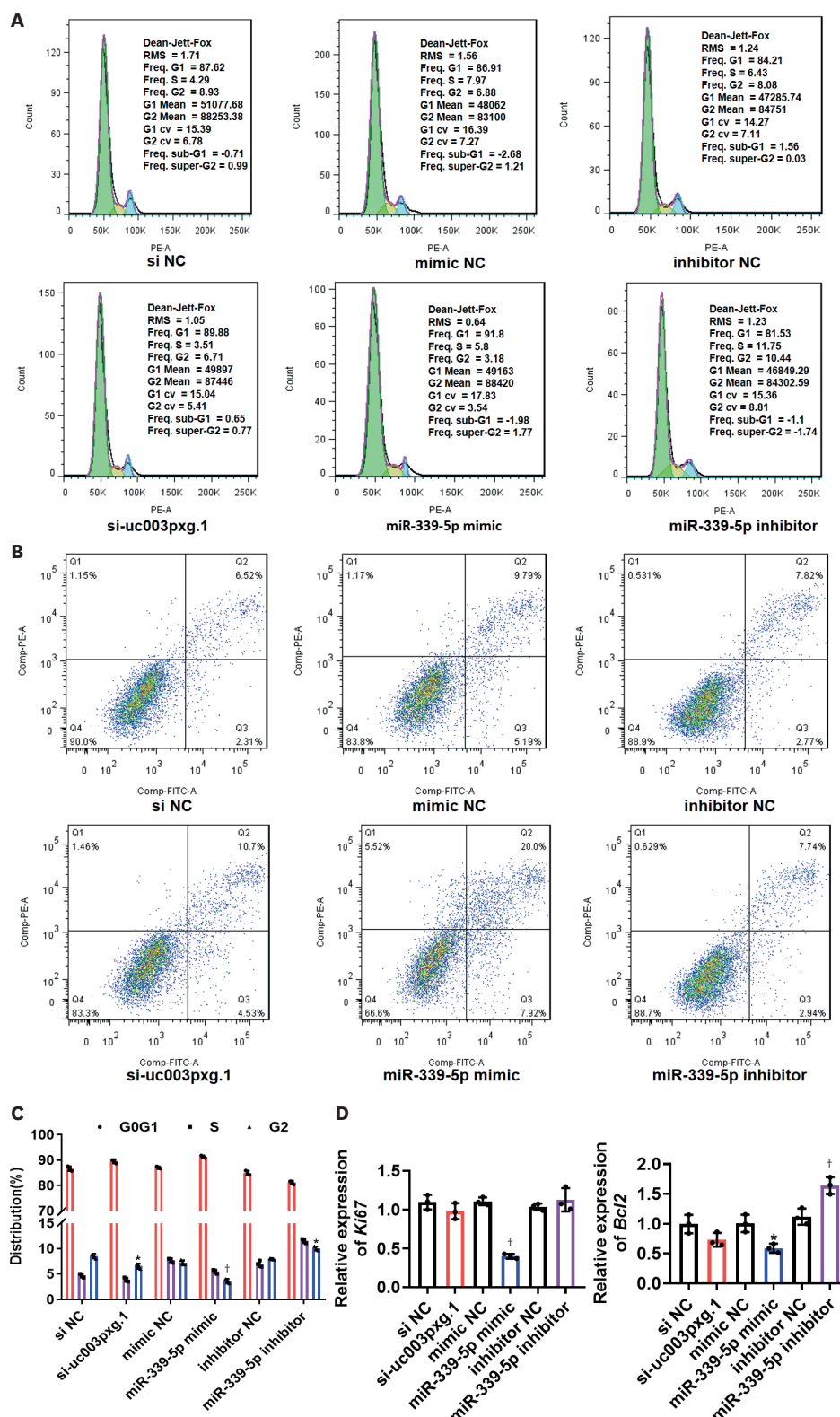


Figure 3. LncRNA uc003pxg.1 and miR-339-5p affected the cell cycle and apoptosis. (A) Flow cytometry was used to analyze the effects of si-uc003pxg.1, miR-339-5p mimic and miR-339-5p inhibitor on the cell cycle. (B) Flow cytometry was used to analyze the effects of si-uc003pxg.1, miR-339-5p mimic and miR-339-5p inhibitor on cell apoptosis. (C) Cell cycle data statistics of (A). (D) The gene expression of *Klf67*, *Bcl2* was detected by reverse transcription-quantitative polymerase chain reaction.

LncRNA = long noncoding RNA; NC = not control.

* $p < 0.05$, † $p < 0.01$.

The vascular tubular formation ability of the miR-339-5p inhibitor group was not significantly different from that of the NC group, both of which had good tubular formation (**Figure 5F and G**). Based on the overall experimental data, we speculate that when harmful stimulation irritates vascular endothelial cells, intracellular uc003pxg.1 expression is upregulated and miR-339-5p expression is downregulated, which then leads to the upregulation of TGF- β 1 and

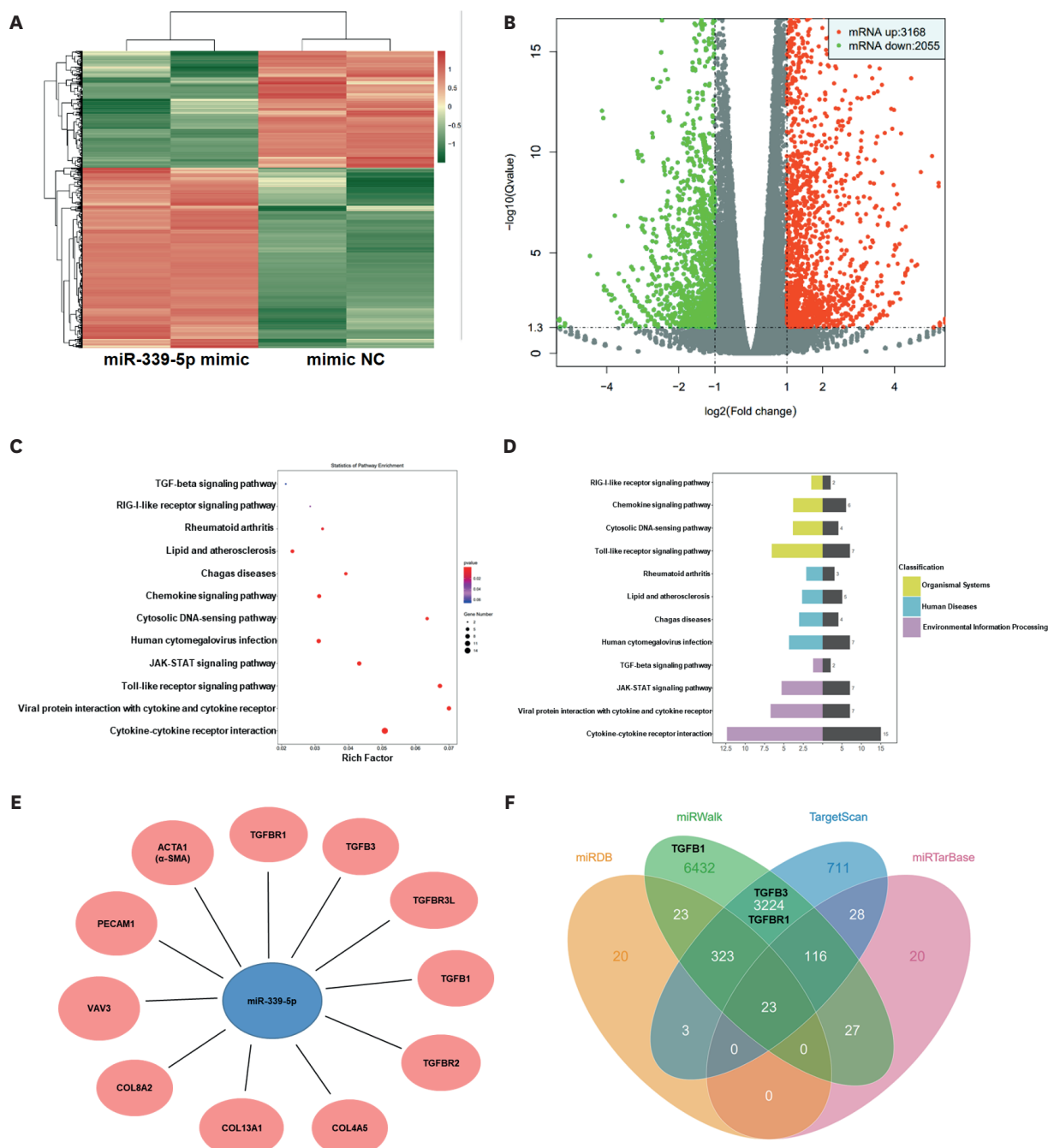


Figure 4. Screening the target gene (TGF- β 1) of miR-339-5p. (A) Cluster analysis showed the differentially expressed genes in the miR-339-5p mimic and NC groups. (B) Volcano map showing upregulated and downregulated genes in the miR-339-5p mimic and NC groups. (C, D) Kyoto Encyclopedia of Genes and Genomes pathway analysis of target genes. (E) Network diagram of miR-339-5p partially downregulated targeted genes. (F) Bioinformatics miRDB, miRwalk, TargetScan and miRTarBase software predicted the target genes of miR-339-5p. NC = not control; TGF- β 1 = transforming growth factor- β 1.

EMT-related genes, such as α -SMA, CD31, collagen III, collagen I and endoglin. Upregulation of these genes can lead to mesenchymal transition and collagen deposition between vascular endothelial cells. Furthermore, upregulation of uc003pxg.1 and downregulation of miR-339-5p also promoted cell proliferation and migration. Cells, collagen and other components of

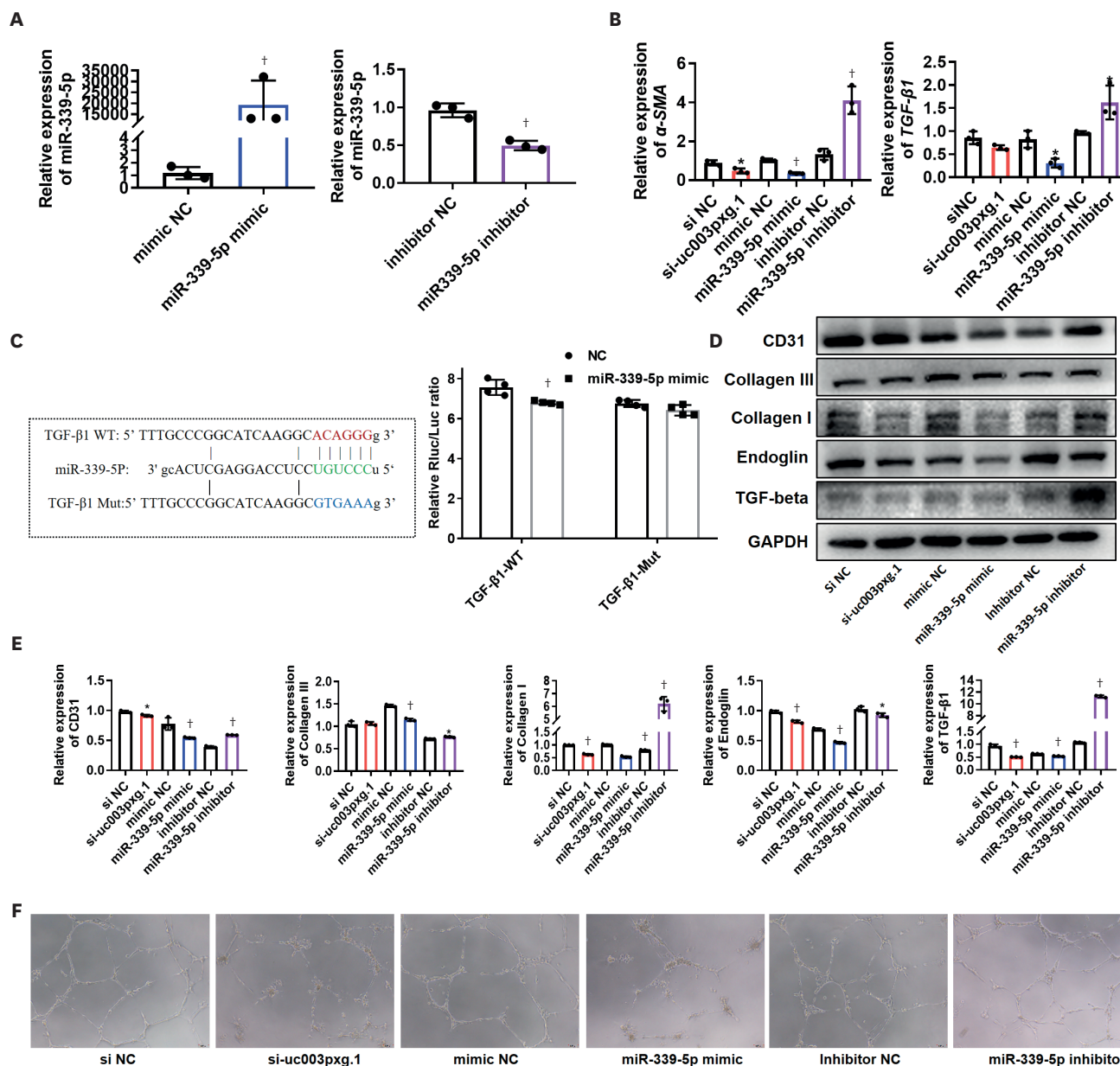


Figure 5. LncRNA uc003pxg.1 and miR-339-5p affect the expression of TGF- β 1, mesenchymal transition collagen-related genes, and it is speculated that they affect the pathogenesis of coronary heart disease. (A) The relative expression of miR-339-5p in HUVECs after transfection with miR-339-5p mimic and inhibitor. (B) Reverse transcription-quantitative polymerase chain reaction was used to detect the expression of TGF- β 1 and α -SMA after HUVECs were transfected with si-uc003pxg.1, miR-339-5p mimic and miR-339-5p inhibitor. (C) Luciferase activities were determined in the miR-339-5p mimic + uc003pxg.1-wt and miR-339-5p mimic + uc003pxg.1-mut groups. (D) The protein expression levels of CD31, collagen III, collagen I, endoglin and TGF- β 1 were detected by western blotting. (E) The gray value statistics of western blotting in (D). (F) Observation of tube formation after si-uc003pxg.1, miR-339-5p mimic and miR-339-5p inhibitor transfection in HUVECs. (G) The branch points statistics of tubes in (F). (H) The mechanism diagram of uc003pxg.1 and miR-339-5p affecting the progression of coronary heart disease.

HUVEC = human umbilical vein endothelial cell; NC = not control; TGF- β 1 = transforming growth factor- β 1; α -SMA = α -smooth muscle actin.

* $p < 0.05$, * $p < 0.01$.

(continued to the next page)

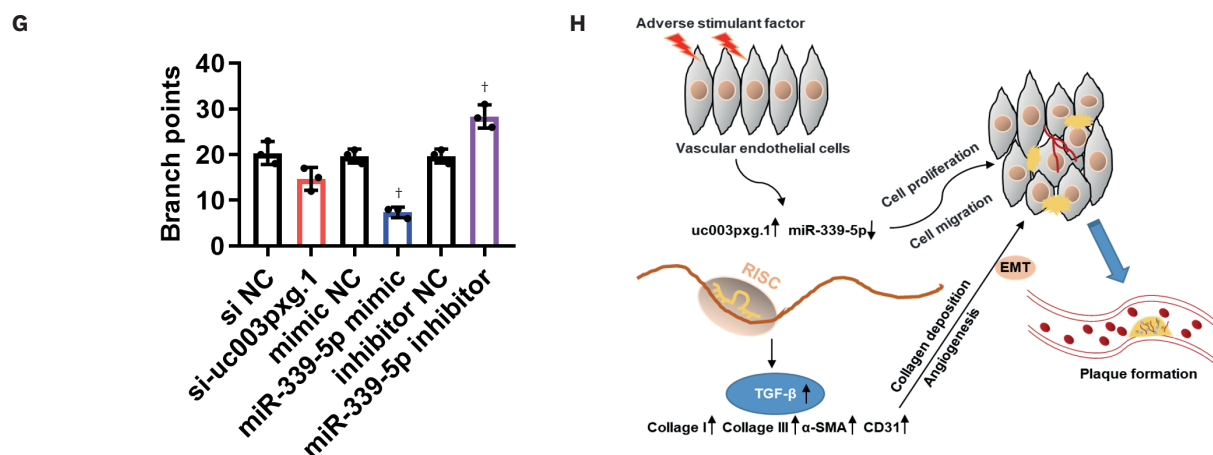


Figure 5. (Continued) LncRNA uc003pxg.1 and miR-339-5p affect the expression of TGF-β1, mesenchymal transition collagen-related genes, and it is speculated that they affect the pathogenesis of coronary heart disease. (A) The relative expression of miR-339-5p in HUVECs after transfection with miR-339-5p mimic and inhibitor. (B) Reverse transcription-quantitative polymerase chain reaction was used to detect the expression of TGF-β1 and α-SMA after HUVECs were transfected with si-uc003pxg.1, miR-339-5p mimic and miR-339-5p inhibitor. (C) Luciferase activities were determined in the miR-339-5p mimic + uc003pxg.1-wt and miR-339-5p mimic + uc003pxg.1-mut groups. (D) The protein expression levels of CD31, collagen III, collagen I, endoglin and TGF-β1 were detected by western blotting. (E) The gray value statistics of western blotting in (D). (F) Observation of tube formation after si-uc003pxg.1, miR-339-5p mimic and miR-339-5p inhibitor transfection in HUVECs. (G) The branch points statistics of tubes in (F). (H) The mechanism diagram of uc003pxg.1 and miR-339-5p affecting the progression of coronary heart disease.

HUVEC = human umbilical vein endothelial cell; NC = not control; TGF-β1 = transforming growth factor-β1; α-SMA = α-smooth muscle actin.

*p<0.05, †p<0.01.

the extracellular environment accumulated in the stimulated point of blood vessels, resulting in the formation or development of vascular plaques (**Figure 5H**).

DISCUSSION

CHD is the leading cause of morbidity and mortality in elderly patients²²⁾ and is estimated to cause more than 23.6 million deaths in 2030.²³⁾ Complex interactions between various cells and inflammation are closely related to the occurrence and development of CHD.²⁴⁾ LncRNAs are important biomarkers and regulators of cardiovascular diseases. However, the expression pattern of circulating lncRNAs in CHD remains poorly understood.²⁵⁾

Studies have shown that miR-339-5p can interact with TGF-β1, and lncRNA NEAT1 can inhibit miR-339-5p to maintain the expression of TGF-β1, thus leading to the occurrence of osteosarcoma.²⁶⁾ TGF-β1 may promote the occurrence of CHD by upregulating sphingosine kinase 1.²⁷⁾ TGF-β1 regulates the migration of VSMCs, and upregulation of endothelin may be necessary in established atherosclerotic plaques.²⁸⁾ Although research on the genetic markers of CHD has not made a breakthrough in reducing the incidence, it can provide a new therapeutic target for the diagnosis and treatment of CHD.²⁹⁾ In addition, lncRNAs promote endothelial angiogenesis.³⁰⁾ The lncRNA uc003pxg.1, which interacts with miR-339-5p, was discovered by high-throughput sequencing in our previous research,²⁰⁾ and we performed an in-depth study in this paper. Clinical sample verification showed that the lncRNA uc003pxg.1 was upregulated in peripheral blood circulating cells of CAD patients (**Figure 1A**), while miR-339-5p was downregulated (**Figure 1B**), and their expression was negatively correlated (**Figure 1C**). A luciferase reporter gene assay also showed that uc003pxg.1 and miR-339-5p interact with each other. EdU, Transwell, CCK-8, cell cycle and apoptosis experiments showed that si-uc003pxg.1 and miR-339-5p mimic significantly decreased cell growth, proliferation and migration, while miR-339-5p inhibitor increased

cell growth, proliferation and migration (**Figures 2 and 3**). To further search for the target downstream genes, we transfected HUVECs with miR-339-5p mimic and NC mimic after high-throughput sequencing. Based on findings in references²⁶⁾ and the results of our bioinformatics analysis, we targeted TGF- β 1 for further study. A luciferase reporter gene assay also showed that miR-339-5p interacts with TGF- β 1 to a certain extent. TGF- β 1, α -SMA, CD31, collagen I, collagen III and endoglin were significantly downregulated after HUVECs were transfected with si-uc003pxg.1 and miR-339-5p mimic and were upregulated in the miR-339-5p inhibitor group (**Figure 5B, D and E, Supplementary Figure 1**). Angiogenesis assays also showed that si-uc003pxg.1 and miR-339-5p mimic weakened the angiogenesis ability of HUVECs, and miR-339-5p inhibitor enhanced it (**Figure 5F and G**). Based on the overall experimental data, we speculate that when vascular endothelial cells suffer from harmful stimulation, uc003pxg.1 is upregulated and miR-339-5p is downregulated, leading to upregulated expression of TGF- β 1, α -SMA, CD31, collagen I, collagen III, and endoglin. In turn, the proliferation and migration ability of cells are enhanced, cell mesenchymal transition is enhanced, and collagen deposition and angiogenesis lead to the formation and development of vascular plaques and promote the development of coronary atherosclerosis (**Figure 5H**).

These findings indicate that lncRNAs and miRNAs can be used as early screening potential biomarkers for the diagnosis of CHD and provide a theoretical research basis for the occurrence and development of plaques. However, our research still has limitations. The study was in the preliminary stage and only had a relatively small sample size. More clinical samples and animal experiments are needed to confirm the mechanism of lncRNAs and miRNAs in future studies.

SUPPLEMENTARY MATERIAL

Supplementary Figure 1

The effect of LncRNA uc003pxg.1 and miR-339-5p on α -SMA and CD31 expression was detected by cellular immunofluorescence assay. Red represents CD31 fluorescence staining, green represents α -SMA fluorescence staining, and blue represents DAPI nuclear staining. The results showed that α -SMA, CD31 were downregulated after HUVECs were transfected with si-uc003pxg.1 and miR-339-5p mimic and were upregulated in the miR-339-5p inhibitor group.

REFERENCES

1. Xu X, Hu H, Lin Y, et al. Differences in leukocyte telomere length between coronary heart disease and normal population: a multipopulation meta-analysis. *BioMed Res Int* 2019;2019:5046867. [PUBMED](#) | [CROSSREF](#)
2. Su Z, Zou Z, Hay SI, et al. Global, regional, and national time trends in mortality for congenital heart disease, 1990-2019: an age-period-cohort analysis for the Global Burden of Disease 2019 study. *EClinicalMedicine* 2022;43:101249. [PUBMED](#) | [CROSSREF](#)
3. Muscella A, Stefano E, Marsigliante S. The effects of exercise training on lipid metabolism and coronary heart disease. *Am J Physiol Heart Circ Physiol* 2020;319:H76-88. [PUBMED](#) | [CROSSREF](#)
4. Schnohr P, Marott JL, Kristensen TS, et al. Ranking of psychosocial and traditional risk factors by importance for coronary heart disease: the Copenhagen City Heart Study. *Eur Heart J* 2015;36:1385-93. [PUBMED](#) | [CROSSREF](#)
5. Wang X, Ouyang Y, Wang Z, Zhao G, Liu L, Bi Y. Obstructive sleep apnea and risk of cardiovascular disease and all-cause mortality: a meta-analysis of prospective cohort studies. *Int J Cardiol* 2013;169:207-14. [PUBMED](#) | [CROSSREF](#)

6. Lüscher TF. Acute and chronic coronary syndromes: coronary dissection, intraplaque haemorrhage, and late lumen loss. *Eur Heart J* 2018;39:3339-42. [PUBMED](#) | [CROSSREF](#)
7. Hu H, Lin Y, Xu X, Lin S, Chen X, Wang S. The alterations of mitochondrial DNA in coronary heart disease. *Exp Mol Pathol* 2020;114:104412. [PUBMED](#) | [CROSSREF](#)
8. Falk E. Pathogenesis of atherosclerosis. *J Am Coll Cardiol* 2006;47:C7-12. [PUBMED](#) | [CROSSREF](#)
9. Stary HC, Chandler AB, Dinsmore RE, et al. A definition of advanced types of atherosclerotic lesions and a histological classification of atherosclerosis. A report from the Committee on Vascular Lesions of the Council on Arteriosclerosis, American Heart Association. *Circulation* 1995;92:1355-74. [PUBMED](#) | [CROSSREF](#)
10. Thum T, Condorelli G. Long noncoding RNAs and microRNAs in cardiovascular pathophysiology. *Circ Res* 2015;116:751-62. [PUBMED](#) | [CROSSREF](#)
11. Philippen LE, Dirks E, Wit JB, Burggraaf K, de Windt LJ, da Costa Martins PA. Antisense microRNA therapeutics in cardiovascular disease: quo vadis? *Mol Ther* 2015;23:1810-8. [PUBMED](#) | [CROSSREF](#)
12. Zhu Y, Yang T, Duan J, Mu N, Zhang T. MALAT1/miR-15b-5p/MAPK1 mediates endothelial progenitor cells autophagy and affects coronary atherosclerotic heart disease via mTOR signaling pathway. *Aging (Albany NY)* 2019;11:1089-109. [PUBMED](#) | [CROSSREF](#)
13. Guo F, Tang C, Li Y, et al. The interplay of lncRNA ANRIL and miR-181b on the inflammation-relevant coronary artery disease through mediating NF-κB signalling pathway. *J Cell Mol Med* 2018;22:5062-75. [PUBMED](#) | [CROSSREF](#)
14. Liu X, Li S, Yang Y, et al. The lncRNA ANRIL regulates endothelial dysfunction by targeting the let-7b/TGF-βR1 signalling pathway. *J Cell Physiol* 2021;236:2058-69. [PUBMED](#) | [CROSSREF](#)
15. Li J, Chen J, Zhang F, et al. LncRNA CDKN2B-AS1 hinders the proliferation and facilitates apoptosis of ox-LDL-induced vascular smooth muscle cells via the ceRNA network of CDKN2B-AS1/miR-126-5p/PTPN7. *Int J Cardiol* 2021;340:79-87. [PUBMED](#) | [CROSSREF](#)
16. Falk E, Nakano M, Bentzon JF, Finn AV, Virmani R. Update on acute coronary syndromes: the pathologists' view. *Eur Heart J* 2013;34:719-28. [PUBMED](#) | [CROSSREF](#)
17. Kattoor AJ, Goel A, Mehta JL. LOX-1: regulation, signaling and its role in atherosclerosis. *Antioxidants (Basel)* 2019;8:218. [PUBMED](#) | [CROSSREF](#)
18. Chen H, Wang Y, Sun B, et al. Negative correlation between endoglin levels and coronary atherosclerosis. *Lipids Health Dis* 2021;20:127. [PUBMED](#) | [CROSSREF](#)
19. Li P, Yan X, Xu G, et al. A novel plasma lncRNA ENST00000416361 is upregulated in coronary artery disease and is related to inflammation and lipid metabolism. *Mol Med Rep* 2020;21:2375-84. [PUBMED](#) | [CROSSREF](#)
20. Li P, Li Y, Chen L, et al. Long noncoding RNA uc003pxg.1 regulates endothelial cell proliferation and migration via miR-25-5p in coronary artery disease. *Int J Mol Med* 2021;48:160. [PUBMED](#) | [CROSSREF](#)
21. Livak KJ, Schmittgen TD. Analysis of relative gene expression data using real-time quantitative PCR and the 2^{-ΔΔCT} method. *Methods* 2001;25:402-8. [PUBMED](#) | [CROSSREF](#)
22. Madhavan MV, Gersh BJ, Alexander KP, Granger CB, Stone GW. Coronary artery disease in patients ≥80 years of age. *J Am Coll Cardiol* 2018;71:2015-40. [PUBMED](#) | [CROSSREF](#)
23. Romano S, Buccheri S, Mehran R, Angiolillo DJ, Capodanno D. Gender differences on benefits and risks associated with oral antithrombotic medications for coronary artery disease. *Expert Opin Drug Saf* 2018;17:1041-52. [PUBMED](#) | [CROSSREF](#)
24. Hansson GK. Inflammation, atherosclerosis, and coronary artery disease. *N Engl J Med* 2005;352:1685-95. [PUBMED](#) | [CROSSREF](#)
25. Hosen MR, Li Q, Liu Y, et al. CAD increases the long noncoding RNA PUNISHER in small extracellular vesicles and regulates endothelial cell function via vesicular shuttling. *Mol Ther Nucleic Acids* 2021;25:388-405. [PUBMED](#) | [CROSSREF](#)
26. Zhang L, Lu XQ, Zhou XQ, Liu QB, Chen L, Cai F. NEAT1 induces osteosarcoma development by modulating the miR-339-5p/TGF-β1 pathway. *J Cell Physiol* 2019;234:5097-105. [PUBMED](#) | [CROSSREF](#)
27. Wang S, Zhang Q, Wang Y, et al. Transforming growth factor β1 (TGF-β1) appears to promote coronary artery disease by upregulating sphingosine kinase 1 (SPHK1) and further upregulating its downstream TIMP-1. *Med Sci Monit* 2018;24:7322-8. [PUBMED](#) | [CROSSREF](#)
28. Ma X, Labinaz M, Goldstein J, et al. Endoglin is overexpressed after arterial injury and is required for transforming growth factor-beta-induced inhibition of smooth muscle cell migration. *Arterioscler Thromb Vasc Biol* 2000;20:2546-52. [PUBMED](#) | [CROSSREF](#)
29. Kessler T, Schunkert H. Coronary artery disease genetics enlightened by genome-wide association studies. *JACC Basic Transl Sci* 2021;6:610-23. [PUBMED](#) | [CROSSREF](#)
30. Leisegang MS, Fork C, Josipovic I, et al. Long noncoding RNA MANTIS facilitates endothelial angiogenic function. *Circulation* 2017;136:65-79. [PUBMED](#) | [CROSSREF](#)